

PII: S0017-9310(96)00142-1

The peculiarities of turbulent heat transfer in electric-arc plasma devices

YU. S. LEVITAN

Moscow State Aviation Institute, Moscow 125871, Russia

(Received 15 November 1995)

Abstract—The well-known experimental data on turbulent heat transfer in a long cylindrical duct (more than 50 diameters long) with d between 5 and 10 mm at flow rates G from 0.1 to 15 g s⁻¹ and currents I from 50 to 400 A are analyzed and correlated. Data on argon flow at pressure p between 0.1 and 2 MPa are worked into equations. Generalization of this data is derived in the form of a dependence between dimensionless turbulent heat conductivity and Reynolds and Hartmann numbers in view of the effect of inertial, viscous and electromagnetic forces. The main sources of turbulent heat conductivity at the indicated conditions are analyzed. It was shown that electromagnetic forces decrease turbulent heat transfer for a fully developed flow with a wall-stabilized d.c. arc. This hypothesis was made to account for the dynamics of transition from laminar to turbulent flow in the above mentioned conditions. The connection between flow regime and departure from local thermodynamic equilibrium (LTE) is established. Copyright © 1996 Elsevier Science Ltd.

1. INTRODUCTION

The different non-stationary regimes in the electric-arc devices with pressures $p = (0.1-10) \times 10^5$ Pa and temperature $T = (7-20) \times 10^3$ K were observed. In many cases these regimes are accompanied by stochastic oscillations of gasdynamic parameters. These oscillations, as a rule, are identified within a turbulent regime.

The investigation of turbulent heat transfer in modern electric-arc energy-consuming devices (e.g. plasma generator, Faraday MHD-generator, MPD-thruster) is important for prediction and determination of efficient control methods of their overall characteristics with the use of external electromagnetic or acoustic fields. The peculiar features of heat transfer in the above mentioned devices are determined by interaction between non-linear Joule heating and turbulent flow when thermal and electrical properties of plasma are drastic functions of state parameters for the most part.

The influence of turbulence on heat transfer can be analysed by using the coefficient of turbulent heat conductivity λ_{turb} , this coefficient may be included into Boussinesq form energy transfer equations for turbulent regimes [1].

This paper is devoted to investigations of physical sources of turbulent heat transfer for a fully developed flow with a wall-stabilized d.c. arc and cocurrent gas flow. The main rules of turbulent heat transfer characteristics in different electric-arc devices can be established only for this case.

Only a very limited number of studies satisfying the above requirements exist, see refs. [2–6]. All these experimental results were obtained in long (more than

40 diameters) segmented cylindrical channels with diameters between 5 and 10 mm and axial supplies of plasma-generating gas (mainly argon) at pressure p from 0.1 to 2 MPa, flow rates G from 0.1 to 15 g s⁻¹ and currents I from 40 to 400 A.

In these works the observed transition from laminar to turbulent flow (with arc voltage fluctuations appearance) was characterized by a number of special properties [7]. The most important of these properties are the following:

- (1) at flow rates greater than 1.5 g s⁻¹, the voltage gradient starts to increase above its laminar value and is enhanced by a factor of 4 at about 15 g s⁻¹;
- (2) the average temperature and its profile do not differ much from the laminar to turbulent case with differing mass flow but constant current.

2. TURBULENT HEAT CONDUCTIVITY OF ELECTRIC-ARC PLASMA

For a stationary, fully developed flow of electric-arc plasma in a cylindrical channel with frame of axes (x, r, ϕ) and parameters

$$\mathbf{u} = (u(r), 0, 0); \quad \mathbf{j} = (j_x(r), 0, 0); \quad \mathbf{E} = (E_x, 0, 0) \quad (1)$$

for conditions of axial symmetric and fully developed flow

$$\partial/\partial\phi = 0, \quad \partial/\partial x = 0 \quad (2)$$

energy transfer equations for current regions of

$$\left(\frac{\lambda_{\text{turb}}}{\lambda_{\Sigma}}\right)_b = \left(\frac{E_{\text{turb}}}{E_x} - 1\right) \left(\frac{E_{\text{turb}}}{E_x} - \frac{U}{\bar{\sigma} E_x^2}\right)^{-1} \quad (9)$$

Notice that $R_b \cong (0.8-0.9)R$ for a fully developed arc plasma flow, where R is the radius of the duct. Here $\bar{\sigma}$ and U are the values of σ and U calculated at the bulk temperature \bar{T} . The value $(\lambda_{\text{turb}}/\lambda_{\Sigma})_o$ on the axis of the duct can be obtained from equation (8). With a little manipulation we get

$$\left(\frac{\lambda_{\text{turb}}}{\lambda_{\Sigma}}\right)_o = \left(\frac{E_{\text{turb}o}}{E_x} - 1\right) \left(\frac{E_{\text{turb}o}}{E_x} - \frac{U_o}{\sigma_o E_x^2}\right)^{-1} \quad (10)$$

where axis parameters are marked by indices o .

Immediately near the wall of duct, where $j_x = 0$, the value $(\lambda_{\text{turb}}/\lambda_{\Sigma})$ decreases up to zero on the wall.

The dependence value (9) was used for the generalization of experimental data in refs. [2-6]. For calculation of $\bar{\sigma}$, U and dimensionless numbers Re and Ha the bulk temperature \bar{T} was determined from the relationship, deduced in ref. [8]

$$\bar{T} = T_w + \frac{IE_x - U(\bar{T})\pi R^2}{8\pi\lambda(\bar{T})} \quad (11)$$

where T_w is the wall temperature (it was assumed that $T_w = 500$ K). The dimensionless numbers Re and Ha were calculated from the relationships deduced in ref. [8]

$$Re = \frac{2G}{\pi R \eta(\bar{T})}, \quad Ha = \frac{\mu_o}{\pi R} \left[\frac{I^3}{\pi \eta(\bar{T}) E_x} \right]^{1/2} \quad (12)$$

where $\mu_o = 4\pi \times 10^{-7}$ H m⁻¹ is a magnetic constant, η is viscosity. The values of η , λ and U were taken from refs. [9-12].

Experimental data from refs. [2-6] are shown in Fig. 1 in the form of dependence $(\lambda_{\text{turb}}/\lambda_{\Sigma})_b = f(Re)$ in accordance with equation (9). At $Re > 10^3$ turbulent heat conductivity is increased considerably as it is seen from Fig. 1. The dispersion of the experimental points

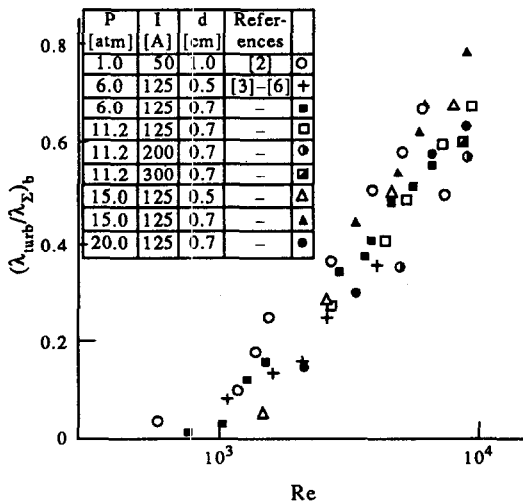


Fig. 1. Function $(\lambda_{\text{turb}}/\lambda_{\Sigma})_b$ vs Reynolds number Re .

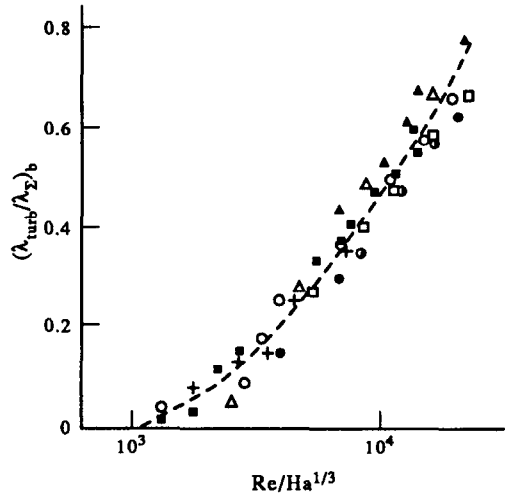


Fig. 2. Function $(\lambda_{\text{turb}}/\lambda_{\Sigma})_b$ vs $Re/Ha^{1/3}$.

may be due to the effect of electromagnetic forces, with current increasing the turbulent heat and conductivity decreasing it. This value hardly affected by pressure or the duct diameter.

Taking into account the effect of electromagnetic forces on turbulent heat conductivity, the same data as in Fig. 1 were replotted in the coordinates $((\lambda_{\text{turb}}/\lambda_{\Sigma})_b, Re/Ha^{1/3})$. As can be seen from Fig. 2, the scatter in the data is smaller than in Fig. 1.

The data in Fig. 2 may be approximated, for example, by the following dependence

$$\begin{aligned} (\lambda_{\text{turb}}/\lambda_{\Sigma})_b \cong & -0.1 + 9.3 \times 10^{-5} M \\ & - 4.4 \times 10^{-9} M^2 + 9.3 \times 10^{-14} M^3, \end{aligned} \quad (13)$$

where $M = Re/Ha^{1/3} \geq 1.15 \times 10^3$.

This dependence is marked by a dotted line in Fig. 2.

3. TURBULENT HEAT CONDUCTIVITY SOURCES IN ELECTRIC-ARC PLASMA

The turbulent electric field strength E_{turb} measured in experiments, contains all the physical sources of turbulent heat transfer in a wall-stabilized arc. For the purpose of the main directed sources let us consider the energy transfer equation for electric-arc plasma flow in a cylindrical duct

$$\rho c_p \left(\frac{\partial T}{\partial t} + U \frac{\partial T}{\partial x} + V \frac{\partial T}{\partial r} \right) = \frac{1}{r} \frac{\partial}{\partial r} \left(r \lambda \frac{\partial T}{\partial r} \right) + \mathbf{j} \cdot \mathbf{E} - U. \quad (14)$$

The current density vector \mathbf{j} is determined, as above, from Ohm's law

$$\mathbf{j} = \sigma \mathbf{E} \quad (15)$$

where ρ and c_p are mass density and heat capacity and u, v are velocity components along the axes x and r .

To obtain a time-averaged equation from equations (14) and (15) a function of both space (\mathbf{r}) and time (t) was expressed in terms of a time-averaged quantity $\langle c \rangle$ and a fluctuating small component c' : $c(\mathbf{r}, t) = \langle c(\mathbf{r}) \rangle + c'(\mathbf{r}, t)$. Substituting these values onto equation (14) taking into account equations (1), (2) and (15) for averaging functions and continuity equation

$$\operatorname{div}(\rho \mathbf{u}) = 0 \quad (16)$$

we get after averaging

$$\begin{aligned} & \frac{1}{r} \frac{d}{dr} \left[r (\langle \lambda \rangle + \lambda_{\text{turb}}) \frac{d\langle T \rangle}{dr} \right] \\ & + \langle \sigma \rangle \langle E_x^2 \rangle \left(1 + \frac{\langle \mathbf{E}'^2 \rangle}{\langle E_x^2 \rangle} + 2 \frac{\langle \sigma' E_x' \rangle}{\langle \sigma \rangle \langle E_x \rangle} \right) \\ & - \langle U \rangle = 0 \quad (17) \end{aligned}$$

where

$$\begin{aligned} \lambda_{\text{turb}} &= \left[\frac{1}{2} \lambda_T \frac{d\langle T^2 \rangle}{dr} - \langle (\rho c_p v)' T' \rangle \right] (d\langle T \rangle / dr)^{-1} \\ \lambda_T &= d\langle \lambda \rangle / d\langle T \rangle. \quad (18) \end{aligned}$$

The time-averaging arc current is

$$\langle I \rangle = 2\pi \int_0^R \sigma_{\text{turb}} \langle E_x \rangle r dr \quad (19)$$

where

$$\sigma_{\text{turb}} = \langle \sigma \rangle \left(1 + \frac{\langle E_x'^2 \rangle}{\langle E_x^2 \rangle} + 2 \frac{\langle \sigma' E_x' \rangle}{\langle \sigma \rangle \langle E_x \rangle} \right). \quad (20)$$

Let us analyze the main physical sources of turbulent heat transfer in a wall-stabilized electric-arc plasma flow for the above mentioned parameters by using these equations and dependencies.

3.1. The effect of electromagnetic forces

As it was established earlier [8], heat transfer in changing from laminar to turbulent flow is determined by the interaction between inertial, viscous and electromagnetic forces. In accordance with this conclusion, heat transfer characteristics of electric-arc plasma flow, specifically, turbulent heat conductivity coefficient, can be represented in the form of a relationship by using dimensionless numbers Re and Ha , which include directed interaction (see Section 2). From this point of view the results of the experiments in refs. [2–6] outlined in Figs. 1 and 2 can be attributed to the effect of electromagnetic forces. The arcing current magnetic field induction increases with arc current increasing, this field value has a maximum on the current-carrying boundary. The inward directed component of electromagnetic force ($j_x B_\phi$) increases, this force retards the cross travel to wall of turbulent 'moles'. In other words, the magnetic field B_ϕ suppresses the cross velocity fluctuations v' resulting in a decrease of the turbulent heat flux component

$\langle (\rho c_p v)' T' \rangle$ as is seen in Figs. 1 and 2. This suppression is not significant since the value of $\langle (\rho c_p v)' T' \rangle$ is too small for a fully developed flow with a wall-stabilized d.c. arc.

It is necessary to stress that a directed effect takes place only for moderate current values, when the wall-stabilizing influence on the arc does not break down. For currents more than the critical value under the present conditions ($\cong 1$ kA) the arc core will occupy the space near the duct axis under the radial electromagnetic force. In this case it is possible that hydro-magnetic instability occurs due to the wall-stabilizing influence decreasing, causing the large-scale fluctuations that in the final analysis lead to the turbulent heat transfer increase [8]. Although these fluctuations are not observed in refs. [2–6] there is a good probability of their arising at small flow rates [8].

The above mentioned suppression of the turbulent transfer in the direction perpendicular to the vector of the magnetic field induction has been much studied as applied to magnetohydrodynamic turbulent flows (see, for example, ref. [13]).

3.2. Electric fluctuations

The appearance of electric fluctuations (electric conductivity σ' , potential ϕ' or electric field strength E' , current density \mathbf{j}' , Joule heating q_v' etc.) due to gasdynamic fluctuations (velocity \mathbf{u}' , temperature T' and pressure p') is an important feature of turbulent electric-arc plasma flows [14, 15]. These fluctuations are included in the one-point correlations $\langle \sigma' \mathbf{E}' \rangle$ and $\langle \mathbf{E}'^2 \rangle$, which appear in the Reynolds-averaged energy transfer equation (17). As shown in refs. [14, 15], these correlations can be expressed in terms of correlations containing electric conductivity fluctuations only for the arc column [14, 15]

$$\begin{aligned} \langle \mathbf{E}'^2 \rangle / \langle E_x^2 \rangle &= (1/3) \langle \sigma'^2 \rangle / \langle \sigma^2 \rangle \\ \langle \sigma' \mathbf{E}' \rangle / (\langle \sigma \rangle \langle \mathbf{E} \rangle) &= -(1/3) \langle \sigma'^2 \rangle / \langle \sigma^2 \rangle. \quad (21) \end{aligned}$$

With regard to these relationships and in accordance to equations (19) and (20) we get the following expressions for σ_{turb} and $\langle I \rangle$

$$\begin{aligned} \sigma_{\text{turb}} &= \langle \sigma \rangle \left(1 - \frac{1}{3} \frac{\langle \sigma'^2 \rangle}{\langle \sigma^2 \rangle} \right) \\ \langle I \rangle &= 2\pi \int_0^R \langle \sigma \rangle \left(1 - \frac{1}{3} \frac{\langle \sigma'^2 \rangle}{\langle \sigma^2 \rangle} \right) \langle E_x \rangle r dr. \quad (22) \end{aligned}$$

From these relationships it is apparent that the appearance of electric conductivity fluctuations (due to the temperature fluctuations in arc column availability) causes the decrease of the time-averaged conductivity and arc current by a factor of $[1 - (1/3)\alpha]$, where $\alpha = \langle \sigma'^2 \rangle / \langle \sigma^2 \rangle$. However, under the test conditions of refs. [2–6] it is obvious that $\langle I \rangle = \text{const.}$ and electric field strength must rise by a factor of $[1 - (1/3)\alpha]^{-1}$ to compensate the conductivity decrease. In this case supplementary turbulent heating

will occur, which produces heat flow and loss increases for the heat transfer equation satisfaction. Hence we obtained the following equation instead of equation (17)

$$\frac{1}{r} \frac{d}{dr} \left[r(\langle \lambda \rangle + \lambda_{\text{turb}}) \frac{d\langle T \rangle}{dr} \right] + \langle \sigma \rangle \langle E_x^2 \rangle \left(1 - \frac{1}{3} \alpha \right)^{-1} - \langle U \rangle = 0. \quad (23)$$

This equation can be used to analyze the influence of electric fluctuations on the turbulent heat conductivity as applied to the fully developed and wall-stabilized arc plasma flow. It is seen from equation (23), that the supplementary turbulent heating and loss in some instances may be caused by electric fluctuations. In electric-arc plasma the temperature fluctuations induce the conductivity fluctuations due to the conductivity-temperature connection availability.

Notice that in the immediate arc core the velocity fluctuations in these conditions are significantly lower than temperature ones because the arc core plasma viscosity is greater than the viscosity of the outer 'cold' gas. Beyond this point the magnetic field damping (see Section 3.1) and wall-stabilizing effect may also promote a decrease in velocity fluctuations. By these means the electric fluctuations can appear initially on the 'laminar background'. Details of the nature and importance of these fluctuations are presented in the next section.

With the availability of electric fluctuations in the arc core for $\langle I \rangle = \text{const.}$ we get $E_{\text{turb}} = \langle E_x \rangle [1 - (1/3)\alpha]^{-1}$, hence the value of E_{turb} varies in the current-carrying duct region directly with variation in the value of $\alpha(r)$ (for small α). After averaging over the cross section of the arc and substituting \bar{E}_{turb} into equation (9) we obtain

$$\left(\frac{\lambda_{\text{turb}}}{\lambda_{\Sigma}} \right)_b = \frac{\bar{\alpha}}{3 - \bar{\alpha}} \left(\frac{3}{3 - \bar{\alpha}} - \frac{\bar{U}}{\sigma E_x^2} \right)^{-1}. \quad (24)$$

The experimental data on temperature fluctuations in the arc core are necessary for numerical estimations of the contribution of electric fluctuations to the turbulent heat conductivity. Unfortunately, the experimental works on the first-hand measurements of the fluctuating parameters arc across section distributions cannot be found. The available modern contact and contactless diagnostic techniques of arc fluctuating characteristics (see ref. [16]) may be used at best to fit the high temperature jets discharged from plasma channels (no more than $(4-7) \times 10^3$ K).

The time-averaged radial distributions of temperature and its fluctuations for laminar and turbulent flows of argon in a segmented channel of diameter $d = 10$ mm and length $L = 136$ mm with a d.c. electric arc have only been investigated in ref. [17].

The operating conditions were: (1) laminar flow—mass flow rate $G = 0.1$ g s⁻¹, and (measured) pressure

level $p \cong 790$ torr (1.04 atm) and (2) turbulent flow— $G = 7.7$ g s⁻¹ and $p \cong 1390$ torr (1.83 atm). Arc current I was 65 A in both cases.

The method itself, representing a combined experimental and analytic technique, is of significance. It is based on the following assumptions: (1) the plasma is in local thermodynamic equilibrium (LTE); (2) the approximation of the optically thin medium is satisfied; (3) the cylindrical symmetry of the arc is retained (in the statistical sense); (4) the plasma is assumed to have a low degree of ionization.

Experimentally, the authors observed the fluctuating radiation from the turbulent arc in the form of the integrated intensity distribution. Through time averaging and inversion (Abel inversion in this work) the time-averaging radial distributions of line and emission coefficients and their mean-square fluctuations were obtained. With this information as inputs to an appropriate analytical formulation the time-averaged radial distributions of temperature and its fluctuations were determined.

In my opinion the least plausible hypothesis in ref. [17] is the assumption of the LTE availability in laminar and particularly turbulent, electric-arc plasma flow. This controversial subject will be discussed in greater detail in the next section.

The estimations of $(\lambda_{\text{turb}}/\lambda_{\Sigma})_b$ value in accordance with the relationship of equation (24) (by using the $\bar{\alpha}$ data from ref. [17]) demonstrate that this quantity is small both for laminar and turbulent regimes: less than 1% for laminar flow and no more than 5% for turbulent flow. The value of $\bar{\alpha}$ was calculated from the formula

$$\bar{\alpha} = \sigma_T^2 \langle \overline{T^2} \rangle / \bar{T}^2, \quad (25)$$

where $\hat{\alpha}_T = d \ln \sigma / d \ln \bar{T}$. In this formula the bulk temperature \bar{T} was calculated from the deduced relationship, equation (11), and the values of $\sigma(T)$ were taken from ref. [18].

The obtained results are realistic as applied to a laminar regime: there will be flattening of the temperature fluctuations because of high argon plasma radiation under experimental conditions. However, these fluctuations are not equal to zero on the arc axis contrary to the results derived from the straightforward gradient models to turbulence [1]. In a turbulent regime the laminar core is also absent, this fact is supported by more detailed numerical investigations [15].

However, experimental results for turbulent flow reported in ref. [17] are contradictory to data in refs. [2-6] and other data in ref. [17]. Really, the values of $(\lambda_{\text{turb}}/\lambda_{\Sigma})_b$ obtained in ref. [17], are no more than 5%, whereas they are nearer 50% according to the dependence equation (9) since $E_{\text{turb}}/\langle E_x \rangle \geq 2$ on evidence derived from ref. [2] by using arc voltages from ref. [17]—76 V for laminar and 260 V for turbulent regimes. This conflicting fact is the subject of the next section.

3.3. Superheat turbulence in electric-arc plasma

The unstable and fluctuating regimes in the free burning nonstabilized arcs appear in the layer between current-carrying and 'cold' gas regions. By contrast, in the section with a fully developed arc plasma flow the dynamic fluctuations are limited by stabilizing and damping effects of the wall and the arcing magnetic field (see Section 3.1). Therefore, in the latter case the main sources of turbulence occur in the arc core.

Generally, in the electric-arc plasma the different instabilities can appear, these instabilities each can give rise to a peculiar kind of turbulence. However, of special interest under the investigated conditions is the superheat instability, which has a maximum increment given in refs. [15, 19]. This increment is equal to $q_{VT}/\rho c_p$, where $q_{VT} = dq_V/dT$, q_V is an intensity of volume heating, for example, Joule heating [19].

The most likely region for superheat instability and associated fluctuating regime appearance ('superheat temperature turbulence' as it is named in ref. [20]) is the high temperature current-conducting channel of the arc, since the directed increment is inversely related to the gas density. As mentioned above, the velocity fluctuations are much less than temperature fluctuations in this region. The resulting data in ref. [17] for the temperature fluctuations in laminar electric-arc plasma flow adds considerable support for this effect.

The electric-arc plasma makes itself evident in passing from a laminar to a turbulent regime. Let us consider this subject by the example of "simple" three-component argon plasma at the investigated conditions. This plasma involves two subsystems—electrons and heavy particles. It has been found [17] that the temperature fluctuations are small in laminar flows for high radiative argon. It is not surprising, then, that these fluctuations cannot lead to the departure from LTE in the arc core [19].

It is well known that the temperature and velocity profiles deform in passing from laminar to turbulent flow. This profile flattening is followed by near wall gradients increasing, with velocity and temperature axes values decreasing. As a result the increasing of the wall shear stress and heat loss takes place. The electrons and heavy particles respond to this profile deformation in various ways. This deformation leads to the electric field strength increase for $\langle I \rangle = \text{const}$. The nature of this effect was discussed in Section 3.2. The electric field acts on electrons largely causing the increase of their kinetic energy and the volume processes intensification. As a result the 'overheating' of electrons in comparison with the heavy particles necessarily leads to the departure from LTE in the current-conducting arc core. Notice that the departure from LTE in the arc core can be observed even with laminar regime for weakly radiative gases (He, H₂) due to more intensive temperature fluctuations in these gases in comparison with high radiative argon. The departure from LTE must be increased for the turbulent regime.

The departure from LTE takes place across the diameter of the duct for turbulent flow [19, 21]. Excess electron energy is transmitted partially to ions and atoms through ambipolar fields and partially by collisions due to turbulent heating. Under these conditions the 'overheating' electrons deform the heavy particles' temperature profile nearer to the initial laminar profile. This effect is supported by the above mentioned fact, that the average temperature and its profile do not differ much from the laminar to turbulent case with differing mass flow but constant current [2-6].

The above mentioned processes dynamics are presented in diagram form in Fig. 3, the temperature profiles of heavy particles T_a and electrons T_e are shown schematically. It must be emphasized that the basis for the execution of this sequence of processes is the superheated electron turbulence which arises. The physics of interaction between electrons and heavy particles has been detailed in ref. [19]. Because of this, the electron subsystem is crucial in turbulent heat

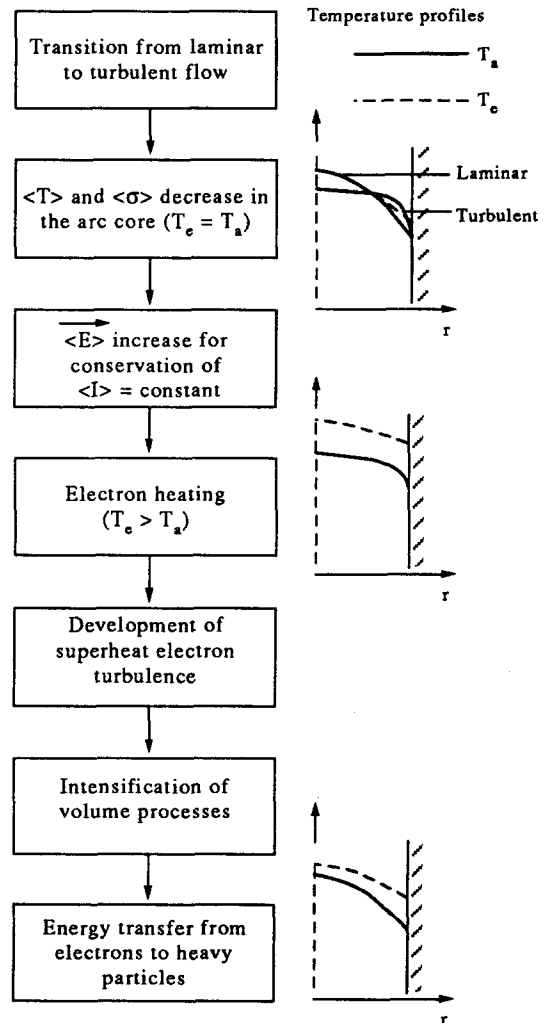


Fig. 3. Qualitative diagram of processes in the section with fully developed electric-arc plasma flow.

transfer, especially in weakly radiative gases. This effect was neglected in ref. [17]—the departure from LTE was not taken into account when applied to the set of equations for turbulent arc plasma. The above directed large discrepancy between the reproduced data from ref. [17] of turbulent heat conductivity from \bar{E}_{turb} measurements and the same data from refs. [2–6], is attributable presumably to neglect of the departure from LTE in ref. [17].

4. CONCLUSION

On the basis of the above data it may be said that the transition from laminar to turbulent flow in the fully developed flow with a wall-stabilized d.c. electric arc must occur simultaneously with transition from equilibrium to nonequilibrium plasma for strongly radiative gases and an increase in the degree of nonequilibrium for weakly radiative gases.

REFERENCES

1. A. S. Monin and A. M. Yaglom, *Statistical Hydro-mechanics*, Part 1. Nauka, Moscow (1965).
2. P. W. Rundstafler Jr, Laminar and turbulent flow of an argon arc plasma. Harvard University, Department of Engineering and Applied Physics, Technical Report, no. 22. (1965).
3. G. Frind, Electric arcs in turbulent flows, 1. ARL report no. 64-148 (1964).
4. G. Frind, Electric arcs in turbulent flows, 2. ARL report no. 66-0073 (1966).
5. G. Frind and B. L. Damsky, Electric arcs in turbulent flows, 3. ARL report no. 68-0067 (1968).
6. G. Frind and B. L. Damsky, Electric arcs in turbulent flows, 4. ARL report no. 70-0001 (1970).
7. I. P. Shkarofsky, Analysis of turbulent flow in wall-stabilized arc discharges. ARL report no. 73-0133 (1973).
8. Yu. S. Levitan, Friction factor and wall heat transfer for laminar and turbulent flow in a cylindrical duct with a wall-stabilized arcs, *IEEE Trans. Plasma Sci.* **20**, 20–33 (1992).
9. R. S. Devoto, Transport coefficients of partially ionized argon. *Phys. Fluids* **10**, 354–364 (1967).
10. J. Kopainsky, Strahlungstransport Mechanismus und transport Koeffizienten im Ar-Hochdruckbogen, *Z. Phys.* **248**, 417–432 (1971).
11. K. S. Drellishak, D. P. Aeschliman and A. B. Cambel, Thermodynamic properties of argon, nitrogen and oxygen plasma. AEDC-TDR 64-12 (1964).
12. N. B. Vargaftik, *Handbook of Physical Properties of Liquids and Gases*. McGraw-Hill, New York (1975).
13. G. G. Branover and A. B. Tzinober, *Magneto-hydrodynamic*. Nauka, Moscow (1970).
14. V. I. Artemov, A. B. Vatazhin, Yu. S. Levitan and O. A. Sinkevich, Approximation of the correlations including pulsations of the electrical parameters on the turbulent flow of high temperature electrically conducting gas, *High Temp. (USA)* **22**, 580–586 (1984).
15. V. I. Artemov, Yu. S. Levitan and O. A. Sinkevich, *Instabilities and Turbulence in Low Temperature Plasma*. Moscow Power Institute, Moscow (1994).
16. M. F. Zhukov, I. M. Zasytkin and Yu. S. Levitan, Experimental studies of electric arcs in turbulent gas flows, *Sov. J. Appl. Phys.* **1**, 26–52 (1987).
17. Y. K. Chien and D. M. Benenson, Temperature diagnostics in turbulent arcs, *IEEE Trans. Plasma Sci.* **8**, 411–417 (1980).
18. R. S. Devoto, Transport coefficients in ionized argon. *Phys. Fluids* **16**, 616–623 (1973).
19. Yu. S. Levitan, Superheat turbulence in gas discharged plasma, *IEEE Trans. Plasma Sci.* **21**, 614–618 (1993).
20. V. I. Artemov, Yu. S. Levitan and O. A. Sinkevich, On superheat temperature turbulence existence. *Pis'ma v Zh. tekhn. fiz.* **10**, 413–416 (1984).
21. A. I. Ivlyutin and Yu. S. Levitan, On LTE in gas discharged turbulent plasma, *Fiz. Plasm i* **17**, 720–727 (1991).